

Correlated interaction effects in an anisotropic flat band fermion system

Jing-Rong Wang^{1,*} and Chang-Jin Zhang^{1,2,†}

¹*High Magnetic Field Laboratory of Anhui Province,
Chinese Academy of Sciences, Hefei 230031, China*

²*Institute of Physical Science and Information Technology, Anhui University, Hefei 230601, China*

An anisotropic flat band fermion system with a novel dispersion that is linear along one direction and cubic along another is proposed in Phys. Rev. X. 13, 021012 (2023). We study the effects of Coulomb interaction in this fermion system by renormalization group theory and Dyson-Schwinger gap equation. We perform renormalization group analysis and find that fermion velocity is always restored along the direction that the fermions take cubic dispersion originally. Accordingly, the system takes the similar behaviors to the two-dimensional Dirac fermion system with Coulomb interaction in the low energy regime. Based on Dyson-Schwinger gap equation method, we find that an excitonic gap is generated if the Coulomb strength is large enough, and the system becomes a novel excitonic Chern insulator with quantized anomalous Hall conductivity. Observable quantities of this system in free case, under weak and strong enough Coulomb interaction are all analyzed.

Introduction. Dirac materials attract extensive studies in the past two decades [1–9]. Graphene is a typical two-dimensional (2D) Dirac semimetal [1–4]. The surface state of three-dimensional (3D) topological insulator is another typical 2D Dirac semimetal [3–6]. For 2D Dirac semimetal, the Fermi surface is discrete point and density of states takes the behavior $\rho(\omega) \propto \omega$, which vanishes at the Fermi level, i.e. $\rho(0) = 0$. Accordingly, the theoretical studies showed that short-range four-fermion interactions are irrelevant if the interactions are weak, but could drive various quantum phase transitions if the interactions are strong enough [2, 10, 11]. Whereas, the Coulomb interaction is long-ranged due to the vanishing of density of states. It was shown that Dirac fermion velocity in 2D Dirac semimetal increases logarithmically with lowering of momenta under long-range Coulomb interaction [2, 12–14]. The singular renormalization of fermion velocity has been observed in graphene through many different experiments [15–17]. There has been also experimental evidence for the singular renormalization of fermion velocity for the surface state of 3D topological insulator [18].

Turning some parameter properly, the fermion velocity of Dirac materials becomes to vanish and the band becomes flat [19–30]. For twisted bilayer graphene, the Dirac fermion velocity vanishes if the twist angle between graphene layers is tuned to magic angles [19, 20]. For the surface state of 3D topological insulator, it was shown that the Dirac fermion velocity vanishes if periodic potential is applied [21, 22]. Flat band also emerges in twisted multilayer graphene, twisted transition metal dichalcogenide, and other moire materials [23–29]. For Bernal bilayer graphene and rhombohedral multilayer graphene, the band becomes flat and the energy dispersion of fermions takes the form $E \propto \pm k^N$, where N is number of layers [31–34]. Accordingly, the density of states satisfies $\rho(\omega) \propto \omega^{\frac{2}{N}-1}$, which is obviously enhanced comparing to monolayer graphene. In proper conditions, higher-order van Hove point appears in the

flat band fermion system [35–39].

For a fermion system with flat band, the kinetic energy is suppressed, and thus correlation effects are usually much enhanced [23–30]. Many novel strong correlated phenomena, including Mott insulator [40–42], unconventional superconductivity [43–54], non-Fermi liquid behaviors [55, 56], various quantum phase transitions [23–30], fractional quantum anomalous Hall effect [57–59] *etc.*, are found in the flat band fermion systems.

Recently, Sheffer *et al.* found that an anisotropic flat band emerges in the surface state of 3D topological insulator if C_4 broken periodic potential is imposed properly [60]. They showed that the Dirac fermion velocity holds along one direction and vanishes along another direction. Accordingly, the fermion dispersion is linear along one direction and cubic along the another. They raised a very interesting question about the behaviors of this system if interactions are considered, which yet to be resolved.

In this Letter, we study the influence of Coulomb interaction on this anisotropic flat band fermion system with a linear-cubic fermion dispersion. This fermion system can be also regarded as an anisotropic semimetal state. In this system, the density of states takes the form $\rho(\omega) \propto \omega^{\frac{1}{3}}$ which vanishes at the Fermi level. Thus, the Coulomb interaction in this system is long-ranged, which could induce strong-correlated phenomena.

Influence of long-range Coulomb interaction on various semimetal state attracted broad interest [62–82]. These studies manifest that the results subtly depend on the dispersion of fermions and dimension of the system, and thus need careful analysis. In the following, we study the influence of long-range Coulomb interaction on this anisotropic flat band fermion system by renormalization group (RG) theory [61] and self-consistent Dyson-Schwinger gap equation. We reveal the behaviors of the system not only in presence of weak Coulomb interaction but also with strong Coulomb interaction.

The model. The action of free fermions can be writ-

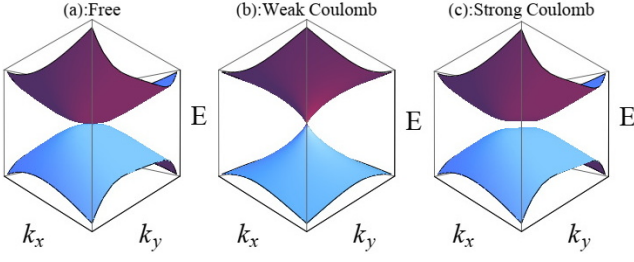


FIG. 1: Fermion dispersion of anisotropic band with linear-cubic fermion (a) in free case, (b) with weak Coulomb interaction becomes, and (c) with strong enough Coulomb interaction.

ten as

$$S_\psi = \int \frac{d\omega}{2\pi} \frac{d^2\mathbf{k}}{(2\pi)^2} \psi^\dagger(-i\omega + \mathcal{H}_f(\mathbf{k})) \psi, \quad (1)$$

where the Hamiltonian for the the fermions is

$$\mathcal{H}_f(\mathbf{k}) = v_x k_x \sigma_1 + d_y k_y^3 \sigma_2. \quad (2)$$

The field operator ψ is a two-component spinor. σ_i with $i = 1, 2, 3$ are the Pauli matrices. v_x and d_y are the model parameters. The fermion energy dispersion is given by

$$E = \pm \sqrt{v_x^2 k_x^2 + d_y^2 k_y^6}, \quad (3)$$

which is linear along one direction, and cubic along another direction.

The Coulomb interaction between fermions takes the form

$$H_C = \frac{1}{4\pi} \int d^2\mathbf{x} d^2\mathbf{x}' \rho(\mathbf{x}) \frac{e^2}{\epsilon |\mathbf{x} - \mathbf{x}'|} \rho(\mathbf{x}'), \quad (4)$$

where $\rho(\mathbf{x}) = \psi^\dagger(\mathbf{x})\psi(\mathbf{x})$ is fermion density operator, e electric charge, and ϵ dielectric constant.

The free fermion propagator reads

$$G_0(\omega, \mathbf{k}) = \frac{1}{-i\omega + v_x k_x \sigma_1 + d_y k_y^3 \sigma_2}. \quad (5)$$

The bare Coulomb interaction is written in the momentum space as

$$V_0(\mathbf{q}) = \frac{2\pi e^2}{\epsilon |\mathbf{q}|} = \frac{2\pi\alpha v}{|\mathbf{q}|}, \quad (6)$$

where $\alpha = e^2/\epsilon v_x$ represents the effective interaction strength.

The polarization is defined as

$$\begin{aligned} \Pi(\Omega, \mathbf{q}) &= - \int \frac{d\omega}{2\pi} \int \frac{d^2\mathbf{k}}{(2\pi)^2} \text{Tr} [G_0(\omega, \mathbf{k}) \\ &\quad \times G_0(\omega + \Omega, \mathbf{k} + \mathbf{q})]. \end{aligned} \quad (7)$$

Substituting the fermion propagator, we find the polarization can be approximately by [83]

$$\begin{aligned} \Pi(\Omega, q_x, q_y) &= \frac{1}{v_x d_y^{\frac{1}{3}}} \left[\frac{c_1 v_x^2 q_x^2}{\left(\Omega^2 + v_x^2 q_x^2 + \frac{c_3^6}{c_2^6} d_y^2 q_y^6\right)^{\frac{5}{6}}} \right. \\ &\quad \left. + \frac{c_3 d_y^{\frac{2}{3}} q_y^2}{\left(\Omega^2 + v_x^2 q_x^2 + \frac{c_3^6}{c_2^6} d_y^2 q_y^6\right)^{\frac{1}{6}}} \right], \end{aligned} \quad (8)$$

where

$$\begin{aligned} c_1 &= \frac{\Gamma\left(\frac{1}{6}\right)}{24 \cdot 2^{\frac{1}{3}} \sqrt{\pi} \Gamma\left(\frac{2}{3}\right)}, & c_2 &= \frac{17}{144}, \\ c_3 &= \frac{9\Gamma\left(\frac{5}{6}\right)}{32 \cdot 2^{\frac{2}{3}} \sqrt{\pi} \Gamma\left(\frac{4}{3}\right)}. \end{aligned} \quad (9)$$

Restoring of fermion velocity. In the following, we analyze the effects of Coulomb interaction through RG method [61]. Firstly, we calculate the fermion self-energy neglecting the screen from polarization function. The fermion self-energy can be written as

$$\Sigma(\omega, \mathbf{k}) = \int \frac{d\Omega}{2\pi} \int' \frac{d^2\mathbf{q}}{(2\pi)^2} G_0(\omega + \Omega, \mathbf{k} + \mathbf{q}) V_0(\Omega, \mathbf{q}) \quad (10)$$

where \int' represents that a momentum shell will be imposed properly. Substituting the propagator of fermion as shown in Eq. (5), and expanding to leading terms of k_x and k_y , we obtain

$$\begin{aligned} \Sigma(\omega, \mathbf{k}) &= -i\omega \Sigma_0 + v_x k_x \sigma_1 \Sigma_1 + d_y k_y^3 \sigma_2 \Sigma_2 \\ &\quad + k_y \sigma_2 \Sigma_L, \end{aligned} \quad (11)$$

where the expressions of $\Sigma_0, \Sigma_1, \Sigma_2, \Sigma_L$ can be found in the Supplementary Materials [83]. We notice that linear term of k_y is always generated dynamically. According, the fermion velocity along y axis is restored.

In order to consider this dynamically generated term in RG analysis, we employ the fermion propagator as following

$$G_0^{new}(\omega, \mathbf{k}) = \frac{1}{-i\omega + v_x k_x \sigma_1 + v_y k_y \sigma_2 + d_y k_y^3 \sigma_2}. \quad (12)$$

The bare value of v_y is taken to be zero in the RG analysis. The fermion self-energy can be written as

$$\begin{aligned} \Sigma(\omega, k) &= \int \frac{d\Omega}{2\pi} \int' \frac{d^2\mathbf{q}}{(2\pi)^2} G_0^{new}(\omega + \Omega, \mathbf{k} + \mathbf{q}) \\ &\quad \times V_0(\Omega, \mathbf{q}). \end{aligned} \quad (13)$$

Substituting the propagator of fermion as shown in Eq. (12), and expanding to the leading terms of ω, k_x and k_y , we arrive

$$\Sigma(\omega, \mathbf{k}) = v_x k_x \sigma_1 C_1 \ell + v_y k_y \sigma_2 C_2^a \ell + d_y k_y^3 \sigma_2 C_2^b \ell \quad (14)$$

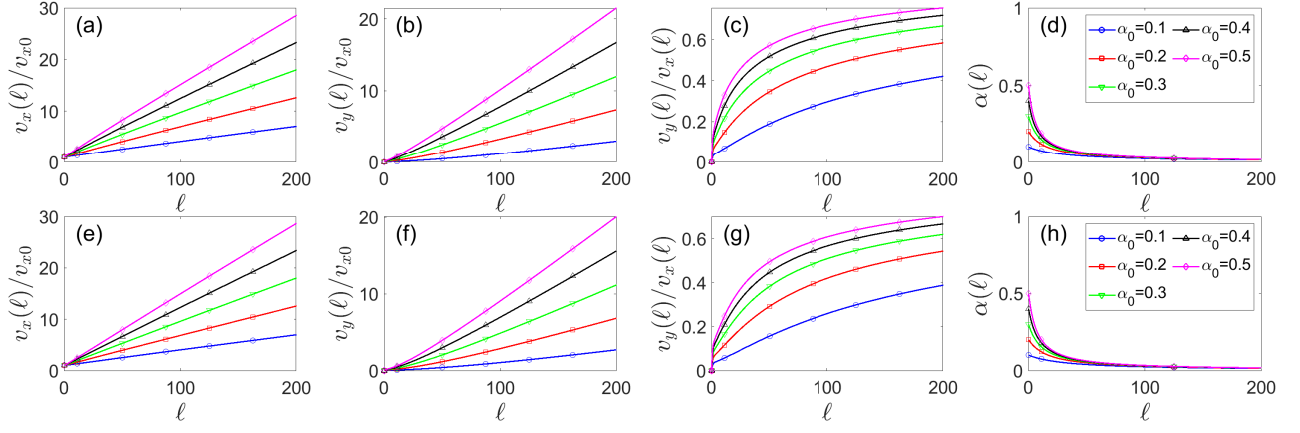


FIG. 2: Flows of $v_x(\ell)$, $v_y(\ell)$, $v_y(\ell)/v_x(\ell)$ and $\alpha(\ell)$ with different initial values of Coulomb strength. (a)-(d) Bare propagator of Coulomb interaction is employed. (e)-(f) Dressed Coulomb interaction is used. Initial value $\beta_0 = 1$ is taken.

C_1 , C_2^a , and C_2^b are functions of the parameters α , β , and γ , which are defined as $\alpha = \frac{e^2}{\epsilon v_x}$, $\beta = \frac{d_y \Lambda^2}{v_x}$, $\delta = v_y/v_x$. The expressions of C_1 , C_2^a , and C_2^b are shown in [83]. The RG scheme $-\infty < \Omega < +\infty$, $b\Lambda < |\mathbf{q}| < \Lambda$ has been utilized, where $b = e^{-\ell}$ with ℓ being the RG running parameter. We get the RG equation as following

$$\frac{dv_x}{d\ell} = C_1 v_x, \quad (15)$$

$$\frac{dv_y}{d\ell} = C_2^a v_y, \quad (16)$$

$$\frac{d\alpha}{d\ell} = -C_1 \alpha. \quad (17)$$

The RG flows of $v_x(\ell)$, $v_y(\ell)$, $v_y(\ell)/v_x(\ell)$, and $\alpha(\ell)$ are shown in Figs. 2(a)-2(d). $v_x(\ell)$ increases nearly linearly with increasing of ℓ . $v_y(\ell)$ grows from zero and also increases nearly linearly with increasing of ℓ . These results indicate that the fermion velocities v_x and v_y acquire logarithmic-like dependence on momenta. The ratio of fermion velocities $v_y(\ell)/v_x(\ell)$ approaches to 1 slowly with increasing of ℓ . The result that $\alpha(\ell)$ flows to zero slowly in the low energy limit $\ell \rightarrow \infty$ represents that Coulomb interaction is marginally irrelevant in the low energy regime.

Subsequently, we calculate the self-energy of fermions considering screen of polarization. In order to consider the original fermion dispersion and the influence of restoring of fermion velocity v_y . We employ the dressed Coulomb interaction as following

$$V^*(\Omega, \mathbf{q}) = \frac{1}{V_0^{-1}(|\mathbf{q}|) + F_1 \Pi(\Omega, \mathbf{q}) + F_2 \Pi_{\text{Dirac}}(\Omega, \mathbf{q})} \quad (18)$$

where $\Pi(\Omega, \mathbf{q})$ is given by (8), and

$$\Pi_{\text{Dirac}}(\Omega, \mathbf{q}) = \frac{1}{16v_x v_y} \frac{v_x^2 q_x^2 + v_y^2 q_y^2}{\sqrt{\Omega^2 + v_x^2 q_x^2 + v_y^2 q_y^2}}, \quad (19)$$

$$F_1 = e^{-\frac{v_y \Lambda}{d_y \Lambda^3}} = e^{-\frac{v_y}{d_y \Lambda^2}}, \quad (20)$$

$$F_2 = e^{-\frac{d_y \Lambda^3}{v_y \Lambda}} = e^{-\frac{d_y \Lambda^2}{v_y}}, \quad (21)$$

where Π_{Dirac} is the polarization induced by 2D Dirac fermions [2]. Considering the dressed Coulomb interaction, the RG equations for v_x and v_y become

$$\frac{dv_x}{d\ell} = (C_1^* - C_0^*) v_x, \quad (22)$$

$$\frac{dv_y}{d\ell} = (C_2^{a*} - C_0^*) v_y, \quad (23)$$

$$\frac{d\alpha}{d\ell} = (-C_1^* + C_0^*) \alpha, \quad (24)$$

where C_0^* , C_1^* , C_2^* , and C_2^{a*} are the functions of α , β , and δ [83]. The RG flows of $v_x(\ell)$, $v_y(\ell)$, $v_y(\ell)/v_x(\ell)$ and $\alpha(\ell)$ considering of screen from polarization functions are shown in Figs. 2(e)-2(h). We can find that these RG flows have the qualitatively same behaviors as the ones shown in Figs. 2(a)-2(d).

Generation of excitonic gap. If the Coulomb interaction is strong enough, an excitonic gap can be generated [84–93]. In order to study the generation of excitonic gap, we employ the Dyson-Schwinger equation method [84–91]. The gap equation to lowest order can be written as

$$\Delta(p_x, p_y) = \frac{1}{2} \int \frac{d^2 \mathbf{k}}{(2\pi)^2} \frac{\Delta(k_x, k_y)}{\sqrt{v_x^2 k_x^2 + d_y^2 k_y^2 + \Delta^2(\omega, k_x, k_y)}} \times V_0(\mathbf{p} - \mathbf{k}). \quad (25)$$

Through numerical calculation, we can find that excitonic gap $\Delta(p_x, p_y)$ is dynamically generated if the Coulomb interaction α is larger enough. Relations between $\Delta(0, 0)$ and α with different values of β are presented in Fig. 3(a). It is easy to notice that $\Delta(0, 0)$ becomes finite if α is larger than a critical value. Dependence of $\Delta(p_x, p_y)$ on p_x and p_y is shown in Fig. 3(b).

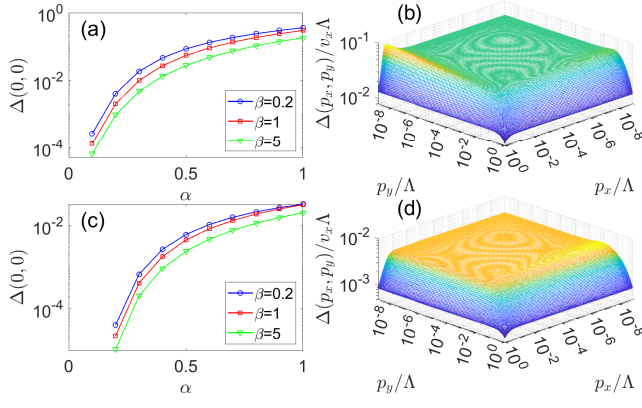


FIG. 3: (a) and (b) $\Delta(0,0)$ and $\Delta(p_x, p_y)$ calculated by bare propagator of Coulomb interaction. (c) and (d) $\Delta(0,0)$ and $\Delta(p_x, p_y)$ calculated by dressed Coulomb interaction including the screen of polarization. In (b) and (d), $\alpha = 0.5$ and $\beta = 1$ are taken.

We find that $\Delta(p_x, p_y)$ approaches to a constant value $\Delta(0,0)$ when p_x and p_y approach to zero. $\Delta(p_x, p_y)$ drops quickly when $v p_x$ or $d_y p_y^3$ is larger than the energy scale given by $\Delta(0,0)$.

Considering the correction from polarization to lowest order, the dressed Coulomb interaction becomes

$$V(\Omega, \mathbf{q}) = \frac{1}{V_0^{-1}(\mathbf{q}) + \Pi(\Omega, \mathbf{q})}, \quad (26)$$

where $\Pi(\Omega, \mathbf{q})$ is given by Eq. (8). Employing the instantaneous approximation [84–86], the Coulomb interaction becomes

$$V(\mathbf{q}) = \frac{1}{V_0^{-1}(\mathbf{q}) + \Pi(0, \mathbf{q})}. \quad (27)$$

Replacing $V_0(\mathbf{q})$ in Eq. (25) with $V(\mathbf{q})$ as shown in Eq. (27), we obtain the gap equation considering the screening from polarization function under instantaneous approximation. Dependence of $\Delta(0,0)$ on α and dependence of $\Delta(p_x, p_y)$ on momenta p_x and p_y considering screen from polarization function are presented in Figs. 3(c) and 3(d) respectively. Comparing Fig. 3(c) with 3(a), and 3(d) with 3(b), we can find that the magnitude of excitonic gap is suppressed if the screening from polarization is considered.

Observable quantities. For free linear-cubic fermion system, the observable quantities including density of states $\rho(\omega)$, specific heat $C_v(T)$, compressibility $\kappa(T)$, diamagnetic susceptibility $\chi_D(T)$, and optical conductivities along the two directions $\sigma_{xx}(\omega)$ and $\sigma_{yy}(\omega)$ take the behaviors [83]

$$\begin{aligned} \rho(\omega) &\propto \omega^{1/3}, & C_v(T) &\propto T^{4/3}, \\ \kappa(T) &\propto T^{1/3}, & \chi_D(T) &\propto T^{-1/3}, \\ \sigma_{xx}(\omega) &\propto \omega^{-2/3}, & \sigma_{yy}(\omega) &\propto \omega^{2/3}, \end{aligned} \quad (28)$$

where ω represents the energy, and T is the temperature.

Under weak Coulomb interaction, the system takes the similar behaviors as 2D Dirac semimetal with Coulomb interaction. Thus, the observable quantities can be written as [2, 94]

$$\begin{aligned} \rho(\omega) &\propto \frac{\omega}{\ln^2\left(\frac{\omega_0}{\omega}\right)}, & C_v(T) &\propto \frac{T^2}{\ln^2\left(\frac{T_0}{T}\right)}, \\ \kappa(T) &\propto \frac{T^2}{\ln^2\left(\frac{T_0}{T}\right)}, & \chi_D(T) &\propto \frac{\ln^2\left(\frac{T_0}{T}\right)}{T}, \\ \sigma_{xx,yy}(\omega) &\propto \sigma_0 \left[1 + \frac{\tilde{C}\alpha}{1 + \alpha \ln\left(\frac{\omega_0}{\omega}\right)} \right]. \end{aligned} \quad (29)$$

If the Coulomb interaction is strong enough, an excitonic gap Δ is generated. Then the observable quantities take the behaviors [83]

$$\begin{aligned} \rho(\omega) &\propto \frac{|\omega|}{(\omega^2 - \Delta^2)^{1/3}} \theta(|\omega| - \Delta), \\ C_v(T) &\propto \frac{\Delta^{10/3}}{T^2} e^{-\frac{\Delta}{T}}, \\ \kappa(T) &\propto \frac{\Delta^{4/3}}{T} e^{-\frac{\Delta}{T}}, \\ \chi(T) &\propto \frac{1}{\Delta^{1/3}}, \\ \sigma_{xx}(\omega) &\propto \frac{1 + 12\frac{\Delta^2}{\omega^2}}{(\omega^2 - 4\Delta^2)^{1/3}} \theta(|\omega| - 2\Delta), \\ \sigma_{yy}(\omega) &\propto (\omega^2 - 4\Delta^2)^{1/3} \left(1 + \frac{20}{3} \frac{\Delta^2}{\omega^2} \right) \theta(|\omega| - 2\Delta) \end{aligned} \quad (30)$$

The behaviors of $C_v(T)$, $\kappa(T)$, and $\chi_D(T)$ are valid in the limit $T \ll \Delta$.

Considering the excitonic gap Δ , the Hamiltonian can be written as

$$\mathcal{H}_\Delta = D_x \sigma_x + D_y \sigma_y + D_z \sigma_z, \quad (31)$$

where the vector \mathbf{D} is defined as

$$\mathbf{D} = v_x k_x \mathbf{e}_x + d_y k_y^3 \mathbf{e}_y + \Delta \mathbf{e}_z. \quad (32)$$

The topological property of this Hamiltonian is determined by the unit vector

$$\hat{\mathbf{D}} = \frac{\mathbf{D}}{|\mathbf{D}|} = \frac{v_x k_x \mathbf{e}_x + d_y k_y^3 \mathbf{e}_y + \Delta \mathbf{e}_z}{\sqrt{v_x^2 k_x^2 + d_y^2 k_y^6 + \Delta^2}}. \quad (33)$$

The corresponding Chern number is given by [95, 96]

$$C = \frac{1}{4\pi} \int d^2 \mathbf{k} \left(\frac{\partial \hat{\mathbf{D}}}{\partial k_x} \times \frac{\partial \hat{\mathbf{D}}}{\partial k_y} \right) \cdot \hat{\mathbf{D}}. \quad (34)$$

Substituting the expression of $\hat{\mathbf{D}}$, we can get

$$\begin{aligned} C &= \frac{1}{4\pi} \int d^2 \mathbf{k} \frac{3v_x d_y k_y^2 \Delta}{[v_x^2 k_x^2 + d_y^2 k_y^6 + \Delta^2]^{3/2}}, \\ &= \frac{1}{2} \text{sgn}(v_x) \text{sgn}(d_y) \text{sgn}(\Delta). \end{aligned} \quad (35)$$

Thus, the system has a quantum anomalous Hall conductivity [95, 96]

$$\sigma_{xy} = C \frac{e^2}{h}, \quad (36)$$

where h is the Planck constant. The system becomes a novel excitonic Chern insulator under strong Coulomb interaction.

Discussion. In summary, we study the influence of long-range Coulomb interaction on an anisotropic flat band fermion with a dispersion which is linear along one direction and cubic along another. Based on RG theory, we show that the fermion velocity is always restored along the direction which has cubic dispersion originally. Accordingly, the system takes the qualitatively same behaviors as the 2D Dirac fermion system with Coulomb interaction. Through self-consistent Dyson-Schwinger gap equation method, we find that the system is driven to excitonic Chern insulator phase if the Coulomb interaction is strong enough.

In Ref. [60], there is a term $k_x^2 k_y \sigma_2$ for the Hamiltonian. In this Letter, we neglect this term to simplify the calculation. Our conclusions will be not changed qualitatively if this term is considered.

Due to vanishing of density of states at the Fermi level, weak four-fermion interaction is irrelevant in the view of RG theory, but strong four-fermion interaction could become relevant and drive the system to a new phase. Considering four-fermion interaction $g_3 (\psi^\dagger \sigma_3 \psi)^2$, through analysis of mean-field method, we find that an excitonic gap Δ is generated if g_3 is larger than a critical value g_{3c} , and it takes the form $\Delta \propto (g_3 - g_{3c})^3$ [83].

Studies about the interplay of Coulomb interaction and short-range four-fermion interaction, and the quantum critical behaviors between the gapless anisotropic band fermion phase and excitonic Chern insulator phase are also interesting.

ACKNOWLEDGEMENTS

We acknowledge the support from National Key R&D Program of China (Grant Nos. 2022YFA1403203, 2024YFA1611103, 2021YFA1600201), the National Natural Science Foundation of China under Grant 12274414, and the Basic Research Program of the Chinese Academy of Sciences Based on Major Scientific Infrastructures (Contract No. JZHKYPT-2021-08).

* Corresponding author: wangjr@hmfl.ac.cn

† Corresponding author: zhangcj@hmfl.ac.cn

[1] A. H. Castro Neto, F. Guinea, N. M. R. Peres, K. S. Novoselov, and A. K. Geim, The electronic properties of graphene, *Rev. Mod. Phys.* **81**, 109 (2009).

- [2] V. N. Kotov, B. Uchoa, V. M. Pereira, F. Guinea, and A. H. Castro Neto, Electron-electron interactions in graphene: Current status and perspectives, *Rev. Mod. Phys.* **84**, 1067 (2012).
- [3] O. Vafek and A. Vishwanath, Dirac fermions in solids: From high- T_c cuprates and graphene to topological insulators and Weyl semimetals, *Annu. Rev. Condens. Matter Phys.* **5**, 83 (2014).
- [4] T. O. Wehling, A. M. Black-Schaffer, and A. V. Balatsky, Dirac materials, *Adv. Phys.* **63**, 1 (2014).
- [5] M. Z. Hasan and C. L. Kane, Colloquium: Topological insulators, *Rev. Mod. Phys.* **82**, 3045 (2010).
- [6] X.-L. Qi and S.-C. Zhang, Topological insulators and superconductors, *Rev. Mod. Phys.* **83**, 1057 (2011).
- [7] N. P. Armitage, E. J. Mele, and A. Vishwanath, Weyl and Dirac semimetals in three-dimensional solids, *Rev. Mod. Phys.* **90**, 015001 (2018).
- [8] B. Q. Lv, T. Qian, and H. Ding, Experimental perspective on three-dimensional topological semimetals, *Rev. Mod. Phys.* **93**, 025002 (2021).
- [9] M. Z. Hasan, G. Chang, I. Belopolski, G. Bian, S.-Y. Xu, J.-X. Yin, Weyl, Dirac and high-fold chiral fermions in topological quantum matter, *Nat. Rev. Mat.* **6**, 784 (2021).
- [10] I. F. Herbut, Interactions and phase transitions on graphene's honeycomb lattice, *Phys. Rev. Lett.* **97**, 146401 (2006).
- [11] I. F. Herbut, V. Juričić, and B. Roy, Theory of interacting electrons on the honeycomb lattice, *Phys. Rev. B* **79**, 085116 (2009).
- [12] J. González, F. Guinea, and M. A. H. Vozmediano, Non-Fermi liquid behavior of electrons in the half-filled honeycomb lattice (A renormalization group approach), *Nucl. Phys. B* **424**, 596 (1994).
- [13] J. Hofmann, E. Barnes, and S. Das Sarma, Why does graphene behave as a weakly interacting system?, *Phys. Rev. Lett.* **113**, 105502 (2014).
- [14] T. Stauber, P. Parida, M. Trushin, M. V. Ulybyshev, D. L. Boyda, and J. Schliemann, Interacting electrons in graphene: Fermi velocity renormalization and optical response, *Phys. Rev. Lett.* **118**, 266801 (2017).
- [15] D. C. Elias, R. V. Gorbachev, A. S. Mayorov, S. V. Morozov, A. A. Zhukov, P. Blake, L. A. Ponomarenko, I. V. Grigorieva, K. S. Novoselov, F. Guinea, and A. K. Geim, Dirac cones reshaped by interaction effects in suspended graphene, *Nat. Phys.* **7**, 701 (2011).
- [16] D. A. Siegel, C.-H. Park, C. Hwang, J. Deslippe, A. V. Fedorov, S. G. Louie, and A. Lanzara, Many-body interactions in quasifreestanding graphene, *Proc. Natl. Acad. Sci. U.S.A.* **108**, 11365 (2011).
- [17] G. L. Yu, R. Jalil, B. Belle, A. S. Mayorov, P. Blake, F. Schedin, S. V. Morozov, L. A. Ponomarenko, F. Chiappini, S. Wiedmann, U. Zeitler, M. I. Katsnelson, A. K. Geim, K. S. Novoselov, and D. C. Elias, Interaction phenomena in graphene seen through quantum capacitance, *Proc. Natl. Acad. Sci. U.S.A.* **110**, 3282 (2013).
- [18] L. Miao, Z. F. Wang, W. Ming, M.-Y. Yao, M. Wang, F. Yang, Y. R. Song, F. Zhu, A. V. Fedorov, Z. Sun, C. L. Gao, C. Liu, Q.-X. Xue, C.-X. Liu, F. Liu, D. Qian, and J.-F. Jia, Quasiparticle dynamics in reshaped helical Dirac cone of topological insulators, *Proc. Natl. Acad. Sci. U.S.A.* **110**, 2758 (2013).
- [19] R. Bistritzer and A. H. MacDonald, Moiré bands in twisted double-layer graphene, *Proc. Natl. Acad. Sci.*

- U.S.A. **108**, 12233 (2011).
- [20] G. Tarnopolsky, A. J. Kruchkov, and A. Vishwanath, Origin of magic angles in twisted bilayer graphene, *Phys. Rev. Lett.* **122**, 106405 (2019).
- [21] J. Cano, S. Fang, J. H. Pixley, and J. H. Wilson, Moiré superlattice on the surface of a topological insulator, *Phys. Rev. B* **103**, 155157 (2021).
- [22] T. Wang, N. F. Yuan, and L. Fu, Moiré surface states and enhanced superconductivity in topological insulators, *Phys. Rev. X* **11**, 021024 (2021).
- [23] E. Y. Andrei and A. H. MacDonald, Graphene bilayers with a twist, *Nat. Mat.* **19**, 1265 (2020).
- [24] L. Balents, C. R. Dean, D. K. Efetov, and A. F. Young, Superconductivity and strong correlations in moiré flat bands, *Nat. Phys.* **16**, 725 (2020).
- [25] S. Carr, S. Fang, and E. Kaxiras, Electronic-structure methods for twisted moiré layers, *Nat. Rev. Mater.* **5**, 748 (2020).
- [26] C. N. Lau, M. W. Bockrath, K. F. Mak, and F. Zhang, Reproducibility in the fabrication and physics of moiré materials, *Nature* **602**, 41 (2022).
- [27] K. F. Mak and J. Shan, Semiconductor moiré materials, *Nat. Nano.* **17**, 686 (2022).
- [28] P. Törmä, S. Peotta, and B. A. Bernevig, Superconductivity, superfluidity and quantum geometry in twisted multilayer systems, *Nat. Rev. Phys.* **4**, 528 (2022).
- [29] K. P. Nuckolls and A. Yazdani, A microscopic perspective on moiré materials, *Nat. Rev. Mater.* **9**, 460 (2024).
- [30] P. A. Pantaleón, A. Jimeno-Pozo, Héctor Sainz-Cruz, V. T. Phong, T. Cea, and F. Guinea, Superconductivity and correlated phases in non-twisted bilayer and trilayer graphene, *Nat. Rev. Phys.* **5**, 304 (2023).
- [31] E. McCann and M. Koshino, The electronic properties of bilayer graphene, *Rep. Prog. Phys.* **75**, 056503 (2013).
- [32] H. Min and A. H. MacDonald, Electronic structure of multilayer graphene, *Prog. Theor. Phys. Suppl.* **176**, 227 (2008).
- [33] M. Koshino and E. McCann, Trigonal warping and Berry's phase $N\pi$ in ABC-stacked multilayer graphene, *Phys. Rev. B* **80**, 165409 (2009).
- [34] F. Zhang, B. Sahu, H. Min, and A. H. MacDonald, Band structure of ABC-stacked graphene trilayers, *Phys. Rev. B* **82**, 035409 (2010).
- [35] A. Shtyk, G. Goldstein, and C. Chamon, Electrons at the monkey saddle: A multicritical Lifshitz point, *Phys. Rev. B* **95**, 035137 (2017).
- [36] N. F. Q. Yuan, H. Isobe, and L. Fu, Magic of high-order van Hove singularity, *Nat. Commun.* **10**, 5769 (2019).
- [37] N. F. Q. Yuan and L. Fu, Classification of critical points in energy bands based on topology, scaling, and symmetry, *Phys. Rev. B* **101**, 125120 (2020).
- [38] A. Chandrasekaran, A. Shtyk, J. J. Betouras, and C. Chamon, Catastrophe theory classification of Fermi surface topological transitions in two dimensions, *Phys. Rev. Research* **2**, 013355 (2020).
- [39] L. Classen and J. J. Betouras, High-order van Hove singularities and their connection to flat bands, *Ann. Rev. Condens. Matter Phys.*, (2025).
- [40] Y. Cao, V. Fatemi, A. Demir, S. Fang, S. L. Tomarken, J. Y. Luo, J. D. Sanchez-Yamagishi, K. Watanabe, T. Taniguchi, E. Kaxiras, R. C. Ashoori, and P. Jarillo-Herrero, Correlated insulator behaviour at half-filling in magic-angle graphene superlattices, *Nature* **556**, 80 (2018).
- [41] G. Chen, L. Jiang, S. Wu, B. Lyu, H. Li, B. L. Chittari, K. Watanabe, T. Taniguchi, Z. Shi, J. Jung, Y. Zhang, and F. Wang, Evidence of a gate-tunable Mott insulator in a trilayer graphene moiré superlattice, *Nat. Phys.* **15**, 237 (2019).
- [42] Y. Tang, L. Li, T. Li, Y. Xu, S. Liu, K. Barmak, K. Watanabe, T. Taniguchi, A. H. MacDonald, J. Shan, and K. F. Mak, Simulation of Hubbard model physics in WSe_2/WS_2 moiré superlattices, *Nature* **19**, 353 (2020).
- [43] Y. Cao, V. Fatemi, S. Fang, K. Watanabe, T. Taniguchi, E. Kaxiras, and P. Jarro-Herrero, Unconventional superconductivity in magic-angle graphene superlattices, *Nature* **556**, 43 (2018).
- [44] M. Yankowitz, S. Chen, H. Polshyn, Y. Zhang, K. Watanabe, D. Graf, A. F. Young, and C. R. Dean, Tuning superconductivity in twisted bilayer graphene, *Science* **363**, 1059 (2019).
- [45] X. Lu, P. Stepanov, W. Yang, M. Xie, M. A. Aamir, I. Das, C. Urgell, K. Watanabe, T. Taniguchi, G. Zhang, A. Bachtold, A. H. MacDonald, and D. K. Efetov, Superconductors, orbital magnets and correlated states in magic-angle bilayer graphene, *Nature* **574**, 653 (2019).
- [46] G. Chen, A. L. Sharpe, P. Gallagher, I. T. Rosen, E. J. Fox, L. Jiang, B. Lyu, H. Li, K. Watanabe, T. Taniguchi, J. Jung, Z. Shi, D. Goldhaber-Gordon, Y. Zhang, and F. Wang, Signatures of tunable superconductivity in a trilayer graphene moiré superlattice, *Nature* **572**, 215 (2019).
- [47] H. S. Arora, R. Polski, Y. Zhang, A. Thomson, Y. Choi, H. Kim, Z. Lin, I. Z. Wilson, X. Xu, J.-H. Chu, K. Watanabe, T. Taniguchi, J. Alicea, and S. Nadj-Perge, Superconductivity in metallic twisted bilayer graphene stabilized by WSe_2 , *Nature* **583**, 379 (2020).
- [48] J. M. Park, Y. Cao, K. Watanabe, T. Taniguchi, and P. Jarillo-Herrero, Tunable strongly coupled superconductivity in magic-angle twisted trilayer graphene, *Nature* **590**, 249 (2021).
- [49] Z. Hao, A. M. Zimmerman, P. Ledwith, E. Khalaf, D. H. Najafabadi, K. Watanabe, T. Taniguchi, A. Vishwanath, and P. Kim, Electric field-tunable superconductivity in alternating-twist magic-angle trilayer graphene, *Science* **371**, 1133 (2021).
- [50] H. Zhou, T. Xie, Takashi, K. Watanabe, and A. F. Young, Superconductivity in rhombohedral trilayer graphene, *Nature* **598**, 434 (2021).
- [51] H. Zhou, L. Holleis, Y. Saito, L. Cohen, W. Huynh, C. L. Patterson, F. Yang, T. Taniguchi, K. Watanabe, and A. F. Young, Isospin magnetism and spin-polarized superconductivity in Bernal bilayer graphene, *Science* **375**, 774 (2022).
- [52] Y. Xia, Z. Han, K. Watanabe, T. Taniguchi, J. Shan, and K. F. Mak, Unconventional superconductivity in twisted bilayer WSe_2 , *Nature* (2024).
- [53] Y. Guo, J. Pack, J. Swann, L. Holtzman, M. Cothrine, K. Watanabe, T. Taniguchi, D. G. Mandrus, K. Barmak, J. Hone, A. J. Millis, A. Pasupathy, and C. R. Dean, Superconductivity in twisted bilayer WSe_2 , arXiv: 2406.03418.
- [54] T. Han, Z. Lu, Y. Yao, L. Shi, J. Yang, J. Seo, S. Ye, Z. Wu, M. Zhou, H. Liu, G. Shi, Z. Hua, K. Watanabe, T. Taniguchi, P. Xiong, L. Fu, and L. Ju, Signatures of chiral Superconductivity in rhombohedral graphene, arXiv:2408.15233.
- [55] H. Polshyn, M. Yankowitz, S. Chen, Y. Zhang, K. Watanabe, T. Taniguchi, C. R. Dean, and A. F. Young,

- Large linear-in-temperature resistivity in twisted bilayer graphene, *Nat. Phys.* **15**, 1011 (2019).
- [56] Y. Cao, D. Chowdhury, D. Rodan-Legrain, O. Rubies-Bigorda, K. Watanabe, T. Taniguchi, T. Senthil, and P. Jarillo-Herrero, Strange metal in magic-angle graphene with near Planckian dissipation, *Phys. Rev. Lett.* **124**, 076801 (2020).
- [57] H. Park, J. Cai, E. Anderson, Y. Zhang, J. Zhu, X. Liu, C. Wang, W. Holtzmann, C. Hu, Z. Liu, T. Taniguchi, K. Watanabe, J.-H. Chu, T. Cao, L. Fu, W. Yao, C.-Z. Chang, D. Cobden, D. Xiao, and X. Xu, Observation of fractionally quantized anomalous Hall effect, *Nature* **622**, 74 (2023).
- [58] F. Xu, Z. Sun, T. Jia, C. Liu, C. Xu, C. Li, Y. Gu, K. Watanabe, T. Taniguchi, B. Tong, J. Jia, Z. Shi, S. Jiang, Y. Zhang, X. Liu, and T. Li, Observation of integer and fractional quantum anomalous Hall effects in twisted bilayer MoTe_2 , *Phys. Rev. X* **13**, 031037 (2023).
- [59] Z. Lu, T. Han, Y. Yao, A. P. Reddy, J. Yang, J. Seo, K. Watanabe, T. Taniguchi, L. Fu, and L. Ju, Fractional quantum anomalous Hall effect in multilayer graphene, *Nature* **626**, 759 (2024).
- [60] Y. Sheffer, R. Queiroz, and A. Stern, Symmetries as the guiding principle for flattening bands of Dirac fermions, *Phys. Rev. X* **13**, 021012 (2023).
- [61] R. Shankar, Renormalization-group approach to interacting fermions, *Rev. Mod. Phys.* **66**, 129 (1994).
- [62] P. Goswami and S. Chakravarty, Quantum criticality between topological and band insulators in 3+1 dimensions, *Phys. Rev. Lett.* **107**, 196803 (2011).
- [63] P. Hosur, S. A. Parameswaran, and A. Vishwanath, Charge transport in Weyl semimetals, *Phys. Rev. Lett.* **108**, 046602 (2012).
- [64] E.-G. Moon, C. Xu, Y. B. Kim, and L. Balents, Non-Fermi-liquid and topological states with strong spin-orbit coupling, *Phys. Rev. Lett.* **111**, 206401 (2013).
- [65] I. F. Herbut and L. Janssen, Topological Mott insulator in three-dimensional systems with quadratic band touching, *Phys. Rev. Lett.* **113**, 106401 (2014).
- [66] B.-J. Yang, E.-G. Moon, H. Isobe, and N. Nagaosa, Quantum criticality of topological phase transitions in three-dimensional interacting electronic systems, *Nat. Phys.* **10**, 774 (2014).
- [67] A. A. Abrikosov, Gapless state of bismuth-type semimetals, *J. Low. Temp. Phys.* **8**, 315 (1972).
- [68] H. Isobe, B.-J. Yang, A. Chubukov, J. Schmalian, and N. Nagaosa, Emergent non-Fermi-liquid at the quantum critical point of a topological phase transition in two dimensions, *Phys. Rev. Lett.* **116**, 076803 (2016).
- [69] G. Y. Cho and E.-G. Moon, Novel quantum criticality in two dimensional topological phase transitions, *Sci. Rep.* **6**, 19198 (2016).
- [70] J.-R. Wang, G.-Z. Liu, and C.-J. Zhang, Excitonic pairing and insulating transition in two-dimensional semi-Dirac semimetals, *Phys. Rev. B* **95**, 075129 (2017).
- [71] H.-H. Lai, Correlation effects in double-Weyl semimetals, *Phys. Rev. B* **91**, 235131 (2015).
- [72] S.-K. Jian and H. Yao, Correlated double-Weyl semimetals with Coulomb interactions: Possible applications to HgCr_2Se_4 and SrSi_2 , *Phys. Rev. B* **92**, 045121 (2015).
- [73] J.-R. Wang, G.-Z. Liu, and C.-J. Zhang, Quantum phase transition and unusual critical behavior in multi-Weyl semimetals, *Phys. Rev. B* **96**, 165142 (2017).
- [74] S.-X. Zhang, S.-K. Jian, and H. Yao, Correlated triple-Weyl semimetals with Coulomb interactions, *Phys. Rev. B* **96**, 241111(R) (2017).
- [75] J.-R. Wang, G.-Z. Liu, and C.-J. Zhang, Breakdown of Fermi liquid theory in topological multi-Weyl semimetals, *Phys. Rev. B* **98**, 205113 (2018).
- [76] J.-R. Wang, G.-Z. Liu, and C.-J. Zhang, Topological quantum critical point in a triple-Weyl semimetal: Non-Fermi-liquid behavior and instabilities, *Phys. Rev. B* **99**, 195119 (2019).
- [77] S. Han, C. Lee, E.-G. Moon, and H. Min, Emergent anisotropic non-Fermi liquid at a topological phase transition in three dimensions, *Phys. Rev. Lett.* **122**, 187601 (2019).
- [78] S.-X. Zhang, S.-K. Jian, and H. Yao, Quantum criticality preempted by nematicity, *Phys. Rev. B* **103**, 165129 (2021).
- [79] B. Roy, M. P. Kennett, K. Yang, and V. Juričić, From birefringent electrons to a marginal or non-Fermi liquid of relativistic spin-1/2 fermions: An emergent superuniversality, *Phys. Rev. Lett.* **121**, 157602 (2018).
- [80] V. N. Kotov, B. Uchoa, and O. P. Sushov, Coulomb interactions and renormalization of semi-Dirac fermions near a topological Lifshitz transition, *Phys. Rev. B* **103**, 045403 (2021).
- [81] Y.-W. Lee and Y.-L. Lee, Correlated second-order Dirac semimetals with Coulomb interactions, *Phys. Rev. B* **105**, 125110 (2022).
- [82] B. Roy and V. Juričić, Correlated fractional Dirac materials, *Phys. Rev. Research* **5**, L032002 (2023).
- [83] See Supplemental Material for the details of the calculation.
- [84] D. V. Khveshchenko, Ghost excitonic insulator transition in layered graphite, *Phys. Rev. Lett.* **87**, 246802 (2001).
- [85] E. V. Gorbar, V. P. Gusynin, V. A. Miransky, I. A. Shovkovy, Magnetic field driven metal-insulator phase transition in planar systems, *Phys. Rev. B* **66**, 045108 (2002).
- [86] G.-Z. Liu, W. Li, and G. Cheng, Interaction and excitonic insulating transition in graphene, *Phys. Rev. B* **79**, 205429 (2009).
- [87] O. V. Gamayun, E. V. Gorbar, and V. P. Gusynin, Gap generation and semimetal-insulator phase transition in graphene, *Phys. Rev. B* **81**, 075429 (2010).
- [88] J.-R. Wang and G.-Z. Liu, Absence of dynamical gap generation in suspended graphene, *New J. Phys.* **14**, 043036 (2012).
- [89] J. González, Phase diagram of the quantum electrodynamics of two-dimensional and three-dimensional Dirac semimetals, *Phys. Rev. B* **92**, 125115(R) (2015).
- [90] M. E. Carrington, C. S. Fischer, L. von Smekal, and M. H. Thoma, Dynamical gap generation in graphene with frequency-dependent renormalization effects, *Phys. Rev. B* **94**, 125102 (2016).
- [91] M. E. Carrington, C. S. Fischer, L. von Smekal, and M. H. Thoma, Role of frequency dependence in dynamical gap generation in graphene, *Phys. Rev. B* **97**, 115411 (2018).
- [92] A. H. Castro Neto, Pauling's dreams for graphene, *Physics* **2**, 30 (2009).
- [93] J. E. Drut and T. A. Lähde, Is graphene in vacuum an insulator, *Phys. Rev. Lett.* **102**, 026902 (2009).
- [94] D. E. Sheekey and J. Schmalian, Quantum critical scaling in graphene, *Phys. Rev. Lett.* **99**, 226803 (2007).
- [95] X.-L. Qi, Y.-S. Wu, and S.-C. Zhang, Topological quan-

tization of the spin Hall effect in two-dimensional paramagnetic semiconductors, *Phys. Rev. B* **74**, 085308 (2006).
[96] C.-X. Liu, S.-C. Zhang, and X.-L. Qi, The quantum

anomalous Hall effect: theory and experiment, *Ann. Rev. Condens. Matter Phys.* **7**, 301 (2016).